SSRG International Journal of Electronics and Communication Engineering
ISSN: 2348-8549/ https://doi.org/10.14445/23488549/IJECE-V12I2P104

Volume 12 Issue 2, 38-53, February 2025

Original Article

Low Coupling Miniaturized MIMO Antenna for Quad Band Application

Ravindra S. Bakale[1], Anil B. Nandgaonkar[2], Mahesh Munde[3], Digambar Puri[4]

[1]*Department of E&TC, College of Engineering, Ambajogai, Maharashtra, India.*
[2]*Department of E&TC, DBATU, Lonere, Raigad, Maharashtra, India.*
[3]*Department of E&TC, St. Xavier's Technical Institute, Mumbai, Maharashtra, India.*
[4]*Department of E&TC, Ramrao Adik Institute of Technology, Navi Mumbai, Maharashtra, India.*

[1]*Corresponding Author : ravindra.bakle@gmail.com*

Received: 06 December 2024 Revised: 04 January 2025 Accepted: 05 February 2025 Published: 26 February 2025

Abstract *- Researchers have recently focused on designing compact MIMO antenna systems for wireless communication with ultra-wideband-however, miniaturization results in weak isolation between antenna elements. Therefore, several isolation enhancement techniques, such as slits, elliptical slots, EBG structure, neutralization lines, decoupling structures, stubs, DGS, and SRR are applied. A compact multi-band and low-coupling antenna is proposed for short-range wireless communication. The design comprises two symmetrical monopole antennae with T-shape stubs to improve the isolation > 18 dB over the 3.1-12GHz. The dimensions of the antenna are 44 x 20 x 1.53 mm3. The quad-band (S11< -10 dB) at 3.25-3.85GHz, 5.10-5.65GHz, 8.60-8.90GHz, and 9.55-11.80GHz is achieved with a mutual coupling (S21) of -22.0dB, -21.36dB, -35dB, and -18dB respectively. The antenna provides effective coverage of four frequency bands with low electromagnetic interference. The antenna with high bandwidth is available for high-frequency applications in the X band. A finite element method solver such as Ansys High-Frequency Structure Simulator (HFSS) software for the design of recommended antennae is preferred. The fabricated antenna was tested using a vector network analyzer to measure S parameters such as S11, S21, and VSWR. The envelope correlation coefficient < .0001, DG > 9.90 dB, CCL < 0.0005 bps/Hz, and TARC <-10dB is obtained over the working bandwidth of the antenna. The actual and measured outcomes approximately match, with a slight deviation due to fabrication, copper, and conductor loss. Therefore, the recommended antenna is the ultimate candidate for multi-band application.*

Keywords *- Diversity gain, Envelope Correlation Coefficient (ECC), MIMO, Mutual coupling, Total active reflection coefficients.*

1. Introduction

Initially, antennas are designed for specific bands such as Wi-max, WLAN, C, and X with low data rates. Recently, there has been a requirement to integrate all bands into a single antenna. However, miniaturization of the antenna is required to implement the new 5G technology. There is a demand for a higher data rate for internet-based services, so multiple-input, multiple-output antennae are proposed. MIMO antennae are designed with isolation > 20dB to achieve better performance for wireless applications. The MIMO antenna design technology studies and applies several isolation techniques to achieve less than -20 dB coupling.

An unlicensed frequency spectrum of 3.1-10.6GHz is allocated for ultra-wideband applications. Wireless communication devices are designed using MIMO antennas to meet the increasing requirements for greater channel capacity and data rates. The antenna mitigates the polarization mismatch and multipath fading effect, enhancing the channel capacity, bandwidth, gain, and diversity performance. Modern handheld devices are incorporated with multiband operational features such as Wi-Fi, Bluetooth, Wi-MAX, WLAN, C, and INSAT. Electromagnetic interference resulted from the MIMO antenna design, which was over 3.1-10.6GHz. Techniques such as notching single/multiple bands are suggested to minimize the EM interference. Electromagnetic band Gap structures of Mushroom type are preferred for band elimination techniques.

2. Literature Survey

A microstrip-fed MIMO antenna for triple-band application was designed with single-band-elimination characteristics. A crescent ring is introduced on two circular patches to notch a band from 3.96-6.2GHz of the proposed structure. Isolation > 16dB is obtained by adding a modified inter-digital capacitor to the ground. Triple bands are generated at 3.08-3.96GHz, 6.2-8.93GHz, and 10-16GHz, covering UWB and Ku bands, respectively. The antenna has moderate miniaturization and electromagnetic interference over impedance bandwidth [1]. A miniaturized triple-band

four-element MIMO antenna using an SRR ring for improved isolation > 22dB was designed to resonate at three bands: 1.95-2.5GHz, 3.15-3.85GHz, and 4.95-6.6GHz [2]. Moderate coupling in the 1.95- 2.5GHz band affects the antenna's performance.

A two-port multiband MIMO antenna for LTE/WLAN and C/X band applications with mutual coupling < -30dB using an EBG structure is proposed. The antenna suffers from Electromagnetic Interference (EM) over the ultra-wideband [3]. A reconfigurable dual wideband wearable MIMO antenna with a hanging resonator was designed to cover frequency bands from 3.11-5.15GHz and 4.81-7.39GHz corresponding to Wi-MAX/ downlink C band and WLAN/uplink C band, respectively. The recommended antenna has poor compactness [4].

The defective ground structure technique achieves mutual coupling of < -19.5dB and < -21dB in dual-band MIMO antenna. A miniaturized MIMO antenna with a triple-band design comprises two 8-shaped monopole antennas on a biomass substrate material. Three sub-section stubs enhance the isolation > 20dB. The triple bands are generated at 2.04-2.51GHz, 4.43-5.35GHz, and 6.76-8.78GHz, respectively, corresponding to WLAN, fixed-mobile, and ITU band applications. The antenna has moderate miniaturization and EM interference among triple-band over 10dB bandwidth [5]. A MIMO antenna with CPW-fed was designed using the rectangular radiator, an L-pattern stub stretched from the radiator, and a strip extension from the ground for Wi-MAX, WLAN, and 5G applications. A meandering neutralization line is loaded between antenna elements to reduce the mutual coupling < -16dB. There is scope for improving the isolation by more than 16dB, which limits the antenna performance, and at the same time, work on miniaturization is also required [6].

The optimization of a MIMO antenna using a meandering monopole with a semicircular radiator for dual-band application is presented. A meandering line resonator reduces the mutual coupling by < -25.3dB by loading it to the ground for the antenna. Better compactness is needed for the designed antenna [7]. A low coupling of < -17dB CPW-fed MIMO antenna for Bluetooth, Wi-Max, and WLAN applications is recommended. Poor miniaturization and moderate mutual coupling are topics of concern for the recommended antenna [8]. A MIMO antenna designed with S11< -10dB over 2.1-11GHz. The carbon black film, which absorbs the interference between two or more elements, reduced mutual coupling by < -15 dB over the entire working bandwidth. High electromagnetic interference and moderate isolation over ultra-wideband are performance-limiting factors for the antenna [9]. A two-element MIMO structure with a triple-band is optimized using two symmetrical monopole antennae for Wi-MAX, WLAN, defense systems, and radio astronomy applications. Neutralization lines and slits decoupling techniques are used to enhance the isolation. The presented antenna has a large size and moderate EM interference over 10dB bandwidth [10]. A triple-band two-element MIMO antenna was optimized at 3.10-3.19GHz, 6.11-6.43GHz, and 7.50-8.04GHz. The antenna comprises two circular patches and rectangular slits. Slots of U-shape are added to the patch to generate a triple band. The dumbbell-pattern structure was added to the ground to minimize the coupling by < -40 dB. Electromagnetic interference and miniaturization are areas of concern for the proposed antenna [11].

A small-size quad-element MIMO antenna was designed for triple-band in sub-6GHz 5G applications. The square patch with rectangular-pattern type slots and circular-shaped slots is used to generate a triple-band at 3.72-3.82GHz, 4.65-4.76GHz, and 6.16-6.46GHz, respectively. The MIMO structure is arranged in a 2x2 configuration with the shared ground so that mutual coupling amongst antenna elements is < -16dB. Narrow bandwidth and moderate isolation are the limiting factors and require improvement for the antenna [12]. A CPW-fed ultra-wideband MIMO antenna designed in a compact size using two antiparallel hexagonal ring radiating elements is presented. High electromagnetic interference and moderate mutual coupling between antenna elements over ultra-wide bands are the topics of concern for the recommended antenna [13]. A stub of circular arc shape is loaded in the ground to maximize the isolation by more than 20dB over 3.1-10.6GHz. A compact MIMO antenna using hexagonal patch elements with a separation of $\lambda 0/31$ between edge-to-edge for multi-band operation at 4.74GHz, 5.88GHz, 6.73GHz, 8.24GHz, and 9.80GHz with coupling < -20dB is designed.

The antenna has poor compactness and moderate EM interference among multi-bands [14]. Dual trapezoidal-shaped radiators with a defected ground structure are presented with mutual coupling < -30dB for dual-band applications. Furthermore, five meander lines are loaded to the structure to improve the isolation further by 17dB. The multi-band is generated at 6.6-7.6GHz and 8.3-10GHz. Electromagnetic interference and isolation > 17dB in the X band requires improvement for the antenna [15]. A miniaturized MIMO structure is designed for an ultra-wide-band application with high isolation. The proposed structure comprises a rectangular monopole with semicircular radiators attached, having an edge-to-edge separation of $0.125\lambda 0$. Elliptical slots and SRR-type structures are introduced in the ground so that $|S21| < -20$ dB over 2.1-12GHz. Moderate electromagnetic interference among multi-bands must be minimized over the impedance bandwidth of the antenna [16].

A staircase hexagonal patch antenna for multi-band operation over 3-37GHz is designed. The electromagnetic interference among eight bands is a significant issue in the antenna design [17]. The Composite Right/Left-Hand unit cell is loaded with a modified square loop antenna to optimize a

miniaturized triple-band MIMO antenna. Moderate coupling is the limitation of the designed antenna and needs to be reduced further over 10dB bandwidth [18]. An ACS-fed compact reconfigurable antenna for GPS, Bluetooth, WLAN, and Wi-Max applications with stable gain and radiation patterns is designed and optimized. The antenna offers a narrow bandwidth, so there is room for improvement. [19]. A fractal MIMO antenna of a hexagonal shape is designed for multi-band operation. The electromagnetic interference among six bands over ultra-widened frequency degrades the antenna's performance and, therefore, must be minimized [20]. A quad-element MIMO antenna using circular radiators with single-band elimination behavior is proposed. A periodic EBG and defective ground structure are integrated into the ground to increase the isolation by > 17.5dB over 10dB Bandwidth. The presented antenna has an impedance BW from 3-16.2GHz with band-notched at 4.6GHz. The antenna has poor compactness and moderate coupling, which are parameters of concern over 3.1-16.2GHz [21].

A small-size two-element dual-band antenna designed at 2.4GHz and 5.5GHz. The monopole antenna consists of dual L-pattern stubs, and an E-pattern strip is added to the dual rectangle-shaped stubs. The DGS and parasitic elements improve the isolation of > 20 dB by loading it to the ground. Moderate EM interference among the dual-band and miniaturization are issued in the presented antenna, so there is room for improvement [22]. A meander line antenna array was designed for dual-band application with isolation > 20dB using a split EBG structure. The antenna offers a narrow bandwidth over the impedance bandwidth, so it is necessary to transform it into wideband or ultra-wideband [23].

Frequency-reconfigurable MIMO antennae are designed using a dual-modifier triangular monopole antenna with Varactor and PIN diodes. Poor miniaturization and high coupling are significant factors of concern for the antenna [24]. A compact UWB MIMO antenna with two-band rejection using tapered microstrip lines fed dual radiating elements on an FR4 substrate is presented. Dual slits of inverted L-shape are added to the patch to eliminate two bands at 5.15-5.85GHz and 6.7-7.1GHz. Isolation>15dB is achieved over the 10 dB BW of 2.9-10.8GHz by loading a T-shaped stub to the ground. Moderate coupling is the performance-limiting parameter of the proposed antenna over the ultra-wideband [25].

A 144 port patch antenna array with dual polarization and poor coupling is designed for Base station application of Massive MIMO at 3.7GHz. The antenna's poor miniaturization is an area of concern [26]. Dual monopole radiators design the proposed structure with isolation by > 18 dB over 3.1-12GHz. The proposed antenna has quad bands at 3.25-3.85GHz, 5.10-5.65GHz, 8.60-8.90GHz, and 9.55-11.80GHz, with improved isolation and better diversity performance characteristics over the quad-band. The antenna comprises three decagon-shaped rings for multiband application, which covers Wi-Max, WLAN, and 5G applications. The antenna is arranged with a suitable orientation so that coupling of less than -30dB is achieved. Electromagnetic interference among multiband is a major issue in the design of antennae [27]. Dual-band elimination characteristics based MIMO antenna optimized using EBG structure for the ultra-wideband application. F-shaped stubs with a counter facing are added to the ground to lower the coupling by -20 dB.

Antenna design complexity is the major area of concern. CSRR and circular disk metasurface MIMO antenna design for C and X band application with a gain of 5.34dB and mutual coupling of less than -55dB over impedance bandwidth is presented. There is a scope for integrating more than two bands in the proposed antenna [28]. A compact dual-band MIMO antenna for 5G applications at 28/38GHz is proposed. Metamaterial array enhances the isolation by more than 28dB over 10dB bandwidth [29].

The novelty of the proposed antenna and existing research work is compared in this section. Electromagnetic simulation software such as CSR, ADS, and HFSS helps to optimize 3D model antenna design so that low coupling, a better radiation pattern, and low reflection are achieved over four frequency bands. The MIMO antenna array configuration for 5G applications can be optimized for improved diversity and high signal-to-noise ratio. Dual orthogonal polarization can be integrated into the design of an antenna that transmits and receives signals simultaneously. Mutual coupling of less than -18 dB is obtained using a T-shaped stub so that interference-less signal reception is achieved. The proposed antenna finds applications for sub-6GHz 5G, satellite communication, and X band.

The paper has been written in different subsections, such as miniaturized multi-band MIMO antenna design and dimensions, which are discussed in section 2. Surface current distribution and simulated S parameters are analyzed in section 3. The fabricated antenna is tested, and results such as S11, S21, diversity performance parameters, and radiation pattern are covered in segment 4. The outcome of the presented antenna is highlighted in segment 5.

3. Proposed Antenna Design

A small-size microstrip-fed multi-band MIMO antenna with better isolation is optimized on an FR4 substrate 44mm x 20mm x 1.53mm, with dimensions having loss tangents of 0.027 and permittivity of 4.4. The proposed antenna contains two symmetrical monopole antennae with a T-pattern stub for multi-band operation over 3.1-12GHz as shown in Figure 1. The four bands are achieved at 3.25-3.85GHz, 5.1-5.65GHz, 8.60-8.90GHz, and 9.55-11.80GHz. The evolution of the presented antenna design over 3.1-12GHz is represented in Figure 2.

Antenna 1 is designed and optimized at f = 9GHz fundamental frequency, as depicted in Figure 2(a). An inverted L-shaped stub of quarter wavelength is added with a microstrip feed of 2mm width. The monopole antenna length is represented by Equation (1).

$$l_{x\,band} = \frac{c}{4\,f_x\sqrt{\varepsilon_{eff}}} \quad (1)$$

$$\text{Where, } \epsilon_{eff} = \frac{(\varepsilon_r+1)}{2} \quad (2)$$

ϵ_{eff} is the effective dielectric constant of the substrate, C is the velocity of Electromagnetic waves in free space at the resonant frequency of the X band, and the respective monopole antenna length at 9GHz. Antenna 1 achieves a frequency band from 8.43-9.51GHz corresponding to the X band. In Figure 2(b), antenna 2 is designed at 8GHz by loading a T-shaped radiator to the feed line. The monopole antenna's length is calculated using Equations (1) and (2). Antenna 2 generates a dual-band from 7.80-8.16GHz and 9.15-10.30GHz. Antenna 3 is designed for the WLAN band using a semicircular arc with the feed line, as depicted in Figure 2(c). The total length of the monopole antenna is given by Equation (3).

$$l_{wlan} = C_{wlan} + L_{wlan} = \frac{c}{4\,f_{wlan}\sqrt{\varepsilon_{eff}}} \quad (3)$$

Where Cwlan highlights the circumference of a semicircular arc and is evaluated by an Equation (4)

$$C_{wlan} = \pi\, R_{wlan} \quad (4)$$

Where Rwlan is the radius of the semicircular arc.

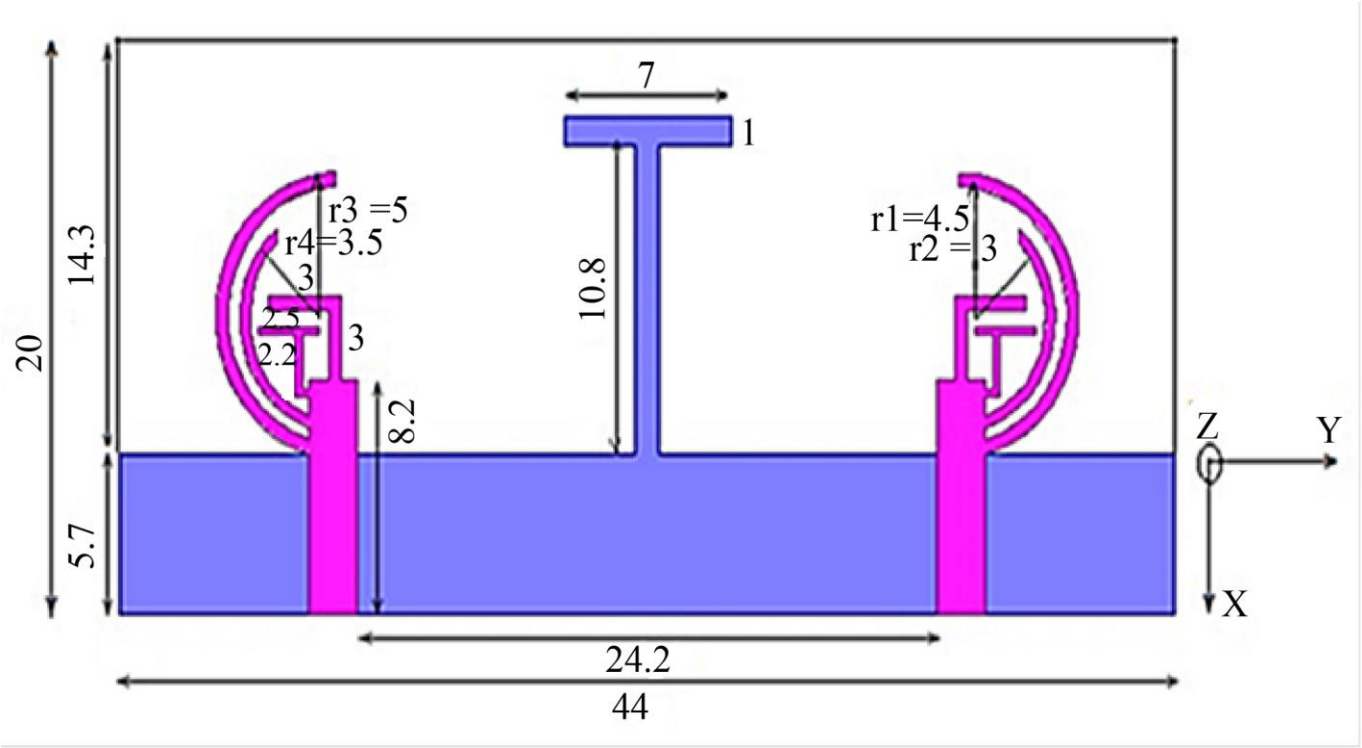

Fig. 1 Recommended antenna with dimensions

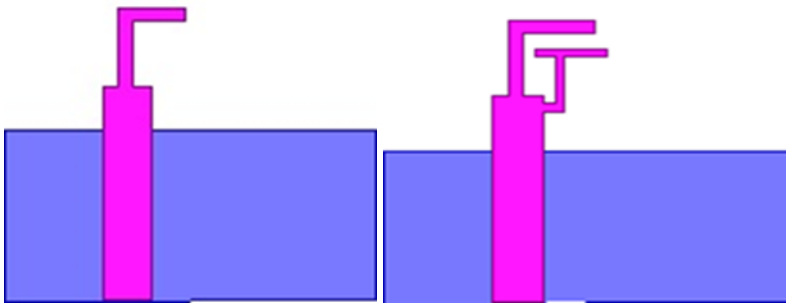

Ant 1 (a) **Ant 2 (b)**

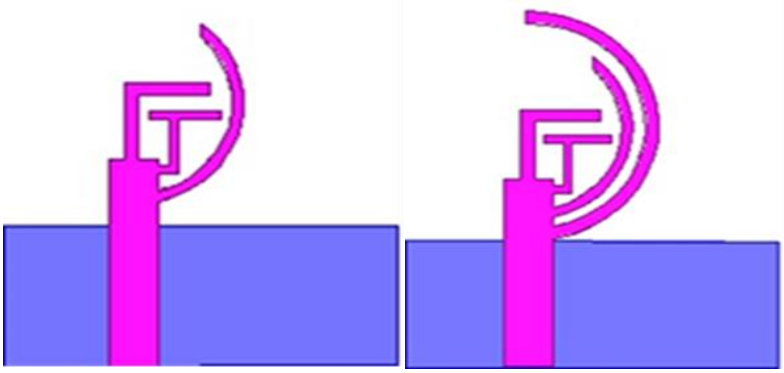

Ant 3 (c) Ant 4 (d)

Fig. 2 Proposed antenna with four bands (a) Single, (b) Dual, (c) Triple, and (d) Quad.

Table 1. Designed specifications of the antenna

Specifications	Unit (mm)	Specifications	Unit (mm)
Substrate Length	44	Substrate Width	20
Ground Length	44	Ground Width	5.7
Length of Feed	8.2	Width of Feed	2
Length for X1 band	14.2	Height of Substrate	1.53
Length for X2 band	12.9	Antenna separation	24.2
Length of Stub	7	Width of Stub	10.8
Length at WLAN	15.18	Radius at WLAN	3.0
Length at Wi-Max	19.28	Radius at Wi-Max	4.5
Circumference of arc at WLAN	9.42	Circumference of arc at Wi-Max	14.13
Permittivity (ϵ_r)	4.4	Size of antenna	44 x 20

Antenna 3 has achieved a triple-band from 4.47-5.64GHz, 7.85-8.48GHz, and 8.84-10.95GHz. Antenna 4 is designed and optimized for the Wi-MAX band using another semicircle arc with a feed line, as depicted in Figure 2(d). Equations (3) and (4) are used to evaluate the Cwi-max and length of Antenna 4, and a quad-band has developed at 3.39-3.93GHz, 5.01-5.62GHz, 8.48-8.70GHz, and 9.02-10.37GHz which is analogous to Wi-MAX, WLAN, and X band respectively. In Table 1, the optimized specifications of the antenna are listed.

3.1. Multi-Software Verification of Antenna

Multi-software verification of the proposed antenna using High-Frequency Structure Simulator (HFSS), Computer Simulation Technology (CST), and Advanced Design System (ADS) over quad-band at 3.25-3.85GHz, 5.15-5.65GHz, 8.60-8.90GHz, and 9.55-11.80GHz are highlighted as follows.

Initially, the HFSS tool is used to design a 3D model of a multiband MIMO antenna. The simulation setup is prepared by assigning suitable boundary conditions, excitation at the port, and a sweep frequency between 3.25 and 11.80 GHz. Antenna impedance matching of 50Ω at every band is verified to ensure low reflection and power loss. Finally, an antenna is simulated, and S parameters S11 and S21 are checked. The performance is analyzed in terms of gain and radiation pattern. Computer Simulation Technology (CST) with an in-built design tool is used to model the proposed antenna. Boundary conditions, excitation at lumped ports, and band frequencies are assigned in the simulation set-up. Validate the antenna and verify results such as S parameter (S11, S21), bandwidth, efficiency, and far-field radiation pattern. ADS is a circuit simulator that can also model 3D antenna designs.

Simulation setup and validation of the antenna are executed in a manner that is very similar to that of CST and HFSS software. If discrepancies are observed, the antenna design is optimized, and simulation results are checked. The performance measuring parameters, such as 10 dB bandwidth, S11, S12, gain, and radiation pattern, are consistent for HFSS, CST, and ADS software.

Lastly, the designed antenna is fabricated and tested using a vector network analyzer in an anechoic chamber. Measured outcomes are compared with the simulated over the multi-frequency band.

4. Discussion on Simulated Results

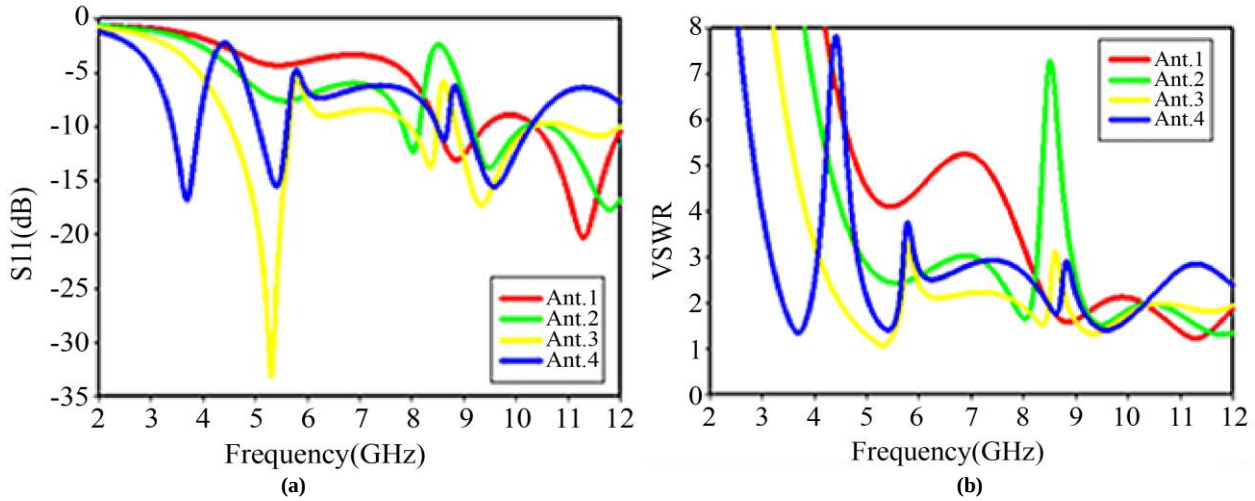

(a) **(b)**

Fig. 3 Simulated outcome (a) S11, and (b) VSWR.

The recommended antenna is simulated using ANSYS HFSS software to measure S11, S21, and VSWR and analyze surface current distribution. The results are presented in Figures 3(a) and 3(b). The simulated outcomes such as |S11| (< -10dB) and |S21| < -18 dB are achieved over 3.1-12GHz. The antenna without stub is shown in Figure 4(a) while with stub in 4(b) respectively. Four bands are achieved at 3.25-3.85GHz, 5.10-5.65GHz, 8.60-8.90GHz, and 9.55-11.80GHz. A T-pattern stub reduces the mutual coupling < -22 dB over 2-8.9GHz, <-18dB from 8.9-10.1GHz, and <-20dB over 10.1-12GHz. Figure 5(a) and 5(b) compare simulated S parameter results for the absence and presence of stubs.

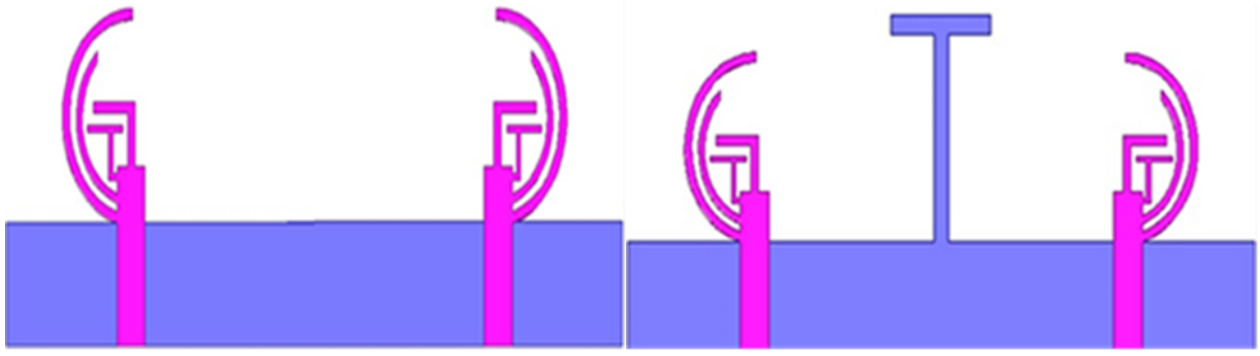

(a) **(b)**

Fig. 4 Isolation enhancement (a) No stub, and (b) With stub.

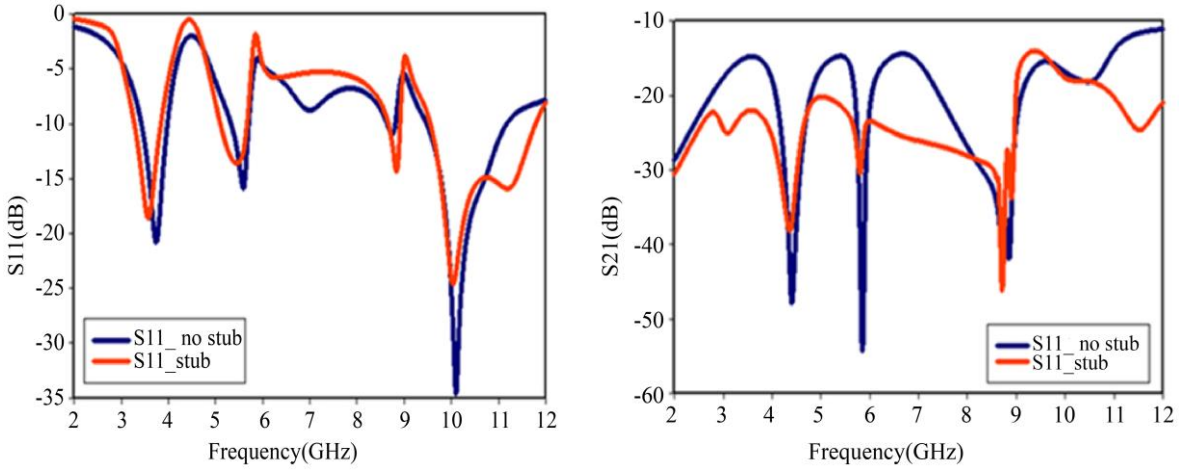

(a) **(b)**

Fig. 5 S parameters for the absence and presence of stubs (a) S11, and (b) S21.

4.1. Isolation Improvement Technique and their Comparison

Each isolation technique has its trade-offs in terms of size, complexity, effectiveness, and cost at different frequencies. The proper selection of isolation method depends on space constraint, amount of mutual coupling required, and frequency range. Split ring resonators, modified IDC, and dumbbell-shaped structures are better for obtaining low coupling at higher frequencies.

Further, Neutralization lines, Split EBG structure, DGS with parasitic elements, strip and open-ended slot, meandering line resonator, and common shared ground are complex in design and applied for high-performance applications. Furthermore, orthogonal placement of antennas, ground stubs, and orientations is a simpler and cost-effective technique for minimum coupling.

Compared with the above method, the proposed T-shaped technique is simpler and more effective for improved isolation of larger than 18 dB across the multiband of the antenna.

4.2. Analysis of Mutual Coupling of the Recommended Antenna

The current distribution over the surface of the recommended antenna measures the isolation enhancement between antenna elements. Port 1 is abolished with a load of 50Ω while Port 2 of the antenna is stimulated. Initially, the MIMO antenna with an absence of a T-shaped stub is simulated at 3.6GHz, 5.5GHz, 8.6GHz, and 10 GHz frequencies, and the results are represented in Figure 6. It is found that the current is coupled to the ground as well as to the adjacent antenna.

The red portion of the antenna highlights the current collected area. Therefore, the isolation of less than 15dB was achieved. A stub of T-shape is added to the ground to analyze simulated surface current distribution results, as plotted in Figure 6. Isolation enhancement of more than 18 dB is achieved. The mutually coupled currents of Antenna 2 are due to the T-shaped stub and Antenna 1. If both currents are out of phase, the current cancels each other, and isolation is enhanced by more than 18 dB for the proposed structure.

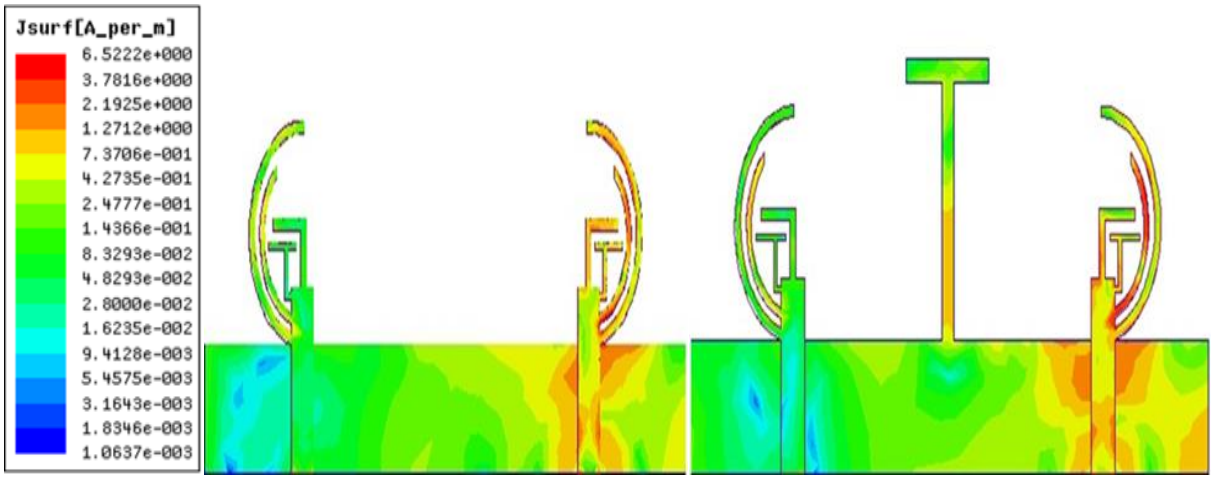

(a) 3.6GHz

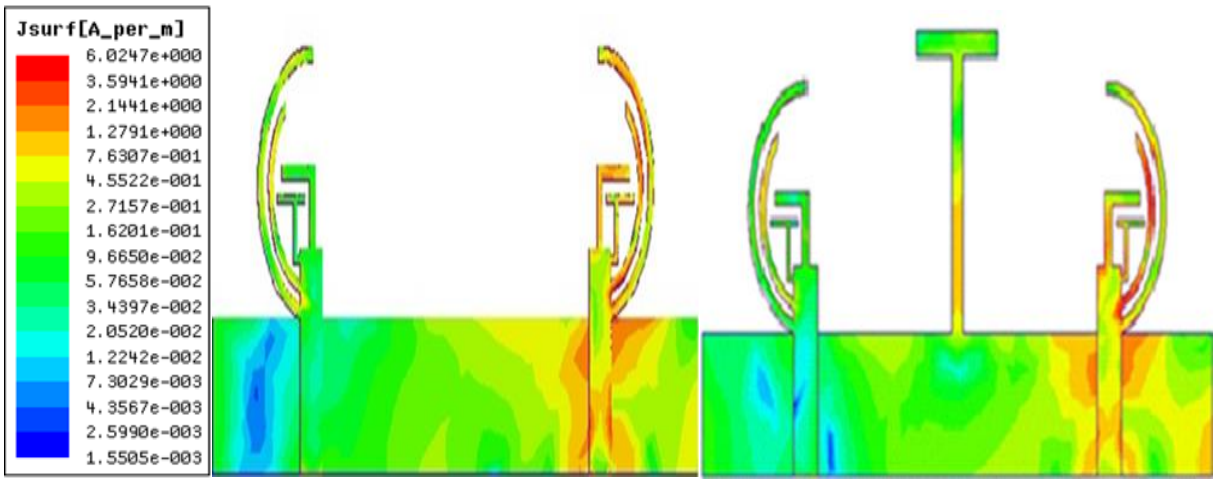

(b) 5.5GHz

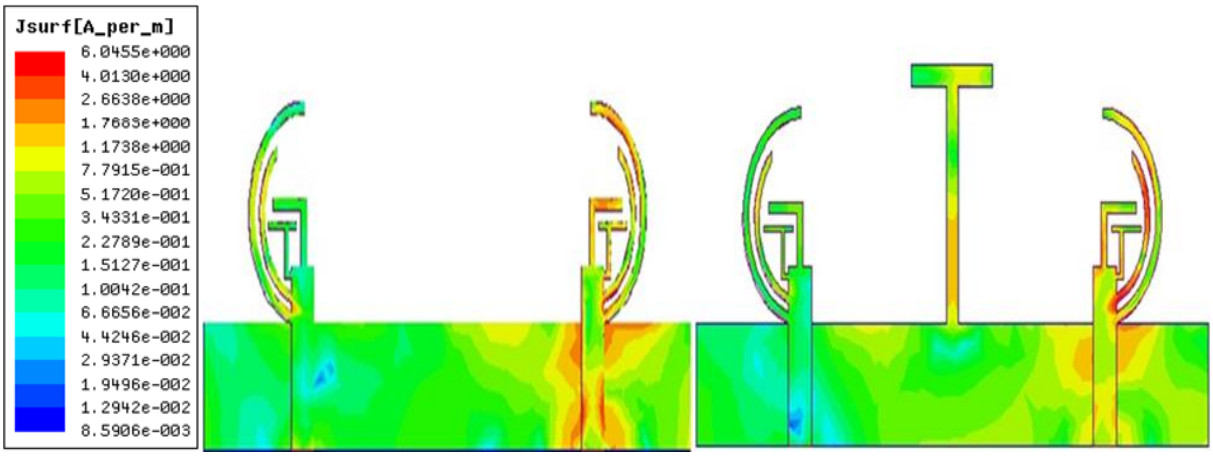

(c) 8.6GHz

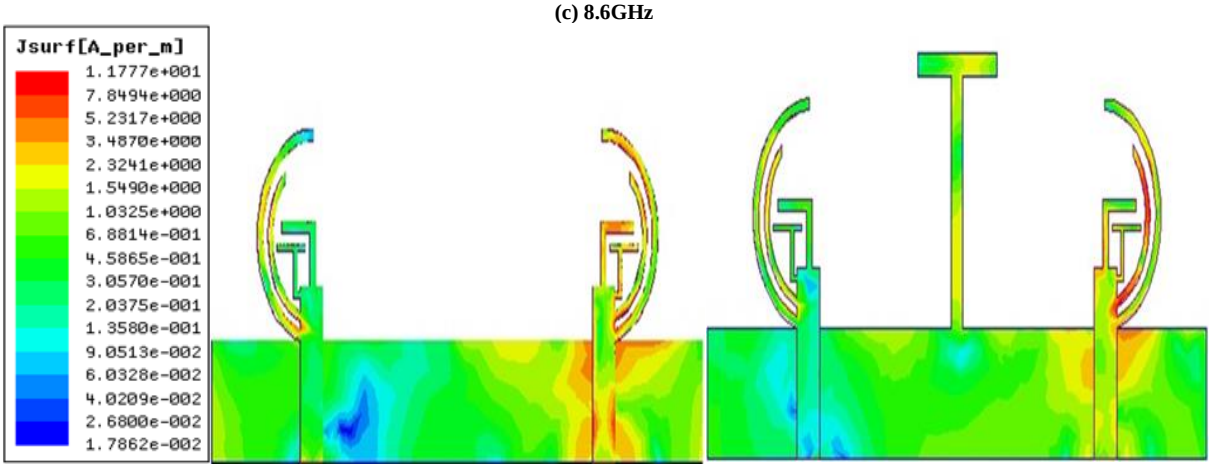

(d) 10GHz

Fig. 6 Mutual couuplng at (a) 3.5GHz, (b) 5.5GHz, (c) 8.6GHz, and (d) 10GHz.

(a) (b)

Fig. 7 Fabricated antenna views (a) Top, and (b) Bottom.

4.3. Mutual Coupling and Antenna Efficiency/Performance Analysis

The antenna's efficiency depends upon the isolation between MIMO antenna elements and, hence, the overall performance of an antenna. For the smaller isolation value, signal interference between antenna elements increases; hence, efficiency, signal-to-noise ratio, and bandwidth are degraded. Similarly, a lower mutual coupling of -18dB over the quad band will enhance the radiation pattern, overall radiation efficiency, and antenna bandwidth. The combination of high efficiency and isolation improves the capacity of the MIMO antenna, enabling the transmission and reception of more data without a major loss of signal-to-noise ratio.

This applies to multi-band MIMO antennas operating at 3.25-3.85GHz, 5.10-5.65GHz, 8.60-8.90GHz, and 9.55-11.80GHz so that each band can operate independently with minimum interference.

5. Testing and Validation of the Fabricated Antenna

Figure 7 highlights the manufactured antenna with a scale comprised of top and bottom views. The Antenna was plotted on an FR4 substrate of 44 x 20 x 1.53 mm3 and is under test using a Vector Network Analyzer N9928A, as depicted in Figure 8.

Fig. 8 MIMO antenna testing using vector network analyzer

5.1 Validation Process of Multiband MIMO Antenna

The following section discusses the validation of the fabricated Multiband MIMO antenna at 3.25- 3.85GHz, 5.10-5.65GHz, 8.6- 8.9GHz, and 9.55- 11.8GHz in terms of graphical representation and statistical analysis for S11, S21, and radiation pattern.

S11 (Return loss): highlight the reflection of the applied signal at the input of the antenna, and the value should be less than -10dB. S11 is plotted over 3.25- 3.85GHz, 5.10-5.65GHz, 8.6-8.9GHz, and 9.55-11.8GHz frequencies with a reflection coefficient less than the threshold level at each frequency band.

S11 is graphically plotted by taking the frequency along the X axis in GHz with S11 along the Y axis in dB. Bandwidth is calculated from the S11 plot whose value is less than -10dB over a frequency band. Statistical performance is evaluated by measuring the average, variance, and standard deviation over the multiband of the antenna.

S21 (isolation between antenna) represents the isolation of a MIMO antenna and should be greater than 18dB over the frequency band. Statistical analysis will help in checking whether isolation is consistent or if any variation occurs. S21 is graphically plotted by taking the frequency along the X axis in GHz with S21 along the Y axis in dB. Mean and median analyze the performance of the antenna statistically.

Radiation pattern: represents the distribution of radiated power from an antenna in different directions. 2D polar radiation patterns represent directivity and gain at a particular frequency. A 3D radiation pattern, either symmetric or directional, is plotted at a different frequency. The antenna's angular coverage is determined using the radiation pattern's Half-Power Beam Width (HPBW). The Cumulative Distribution Function (CDF) of Gain can be used to understand the distribution of gain values across different angles and frequencies. Simulated vs. Measured Data: Measured S11 and S21 and simulated outcomes are analyzed to ensure the fabricated antenna's design specifications are achieved. Simulated and measured S-parameters are graphically plotted over a quad-band of the antenna. Evaluate the error between measured and simulated data for S11 and S21. Statistical analysis of this error using mean and standard deviation can be done to realize the discrepancies.

5.2. Calibration of S Parameters of the Antenna

Table 2 tabulates the measured outcomes of the quad-band at 3.30-3.83GHz, 5.15-5.62GHz, 8.63-8.88GHz, and 9.60-11.65GHz with the improved isolation (S21).

The measured S parameters are compared with the actual results and observed to be in close approximation over the quad-band of the antenna, as represented in Figure 9. The minor variation in both results is because of fabrication, connector, and copper loss.

Table 2. Analysis of actual and calibrated outcomes

Frequency Band (GHz)		Isolation(dB)	
Simulated	**Measured**	**Simulated**	**Measured**
3.25-3.85	3.30-3.83	22.0	24.0
5.10-5.65	5.15-5.62	21.36	20.5
8.60-8.90	8.63-8.88	35.0	32.1
9.55-11.8	9.60-11.65	18.0	17.2

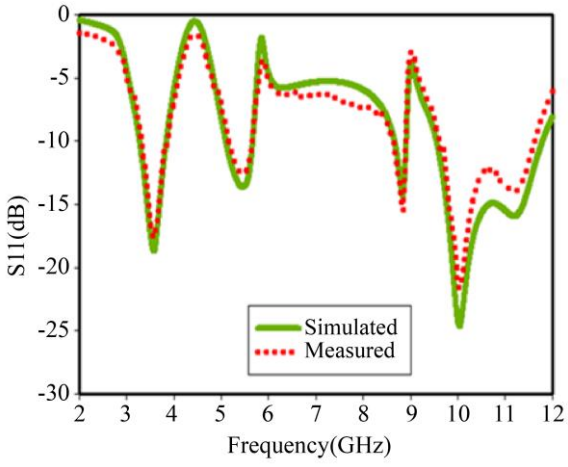

(a)

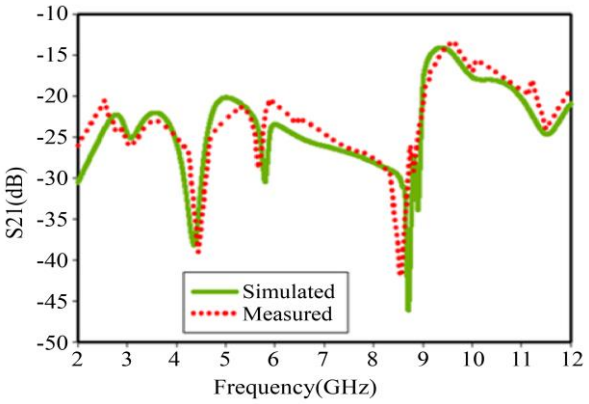

(b)

Fig. 9 Calibration of S specifications (a) S11, and (b) S21.

5.3. Radiation Attributes of the Antenna

The radiation attributes are plotted at 3.6GHz, 5.4GHz, 8.8GHz, and 10.6GHz at φ = 000 and φ = 900, analogous to the X-Z Plane and Y-Z plane, respectively, as depicted in Figure 10.

The measurement is done by terminating one port with a 50Ω load while another port is excited. The bidirectional and omnidirectional radiation patterns are stable over the quad-band of the recommended structure.

The calibrated and actual results are comparatively analyzed over 3.1-12GHz and found to be in better correlation.

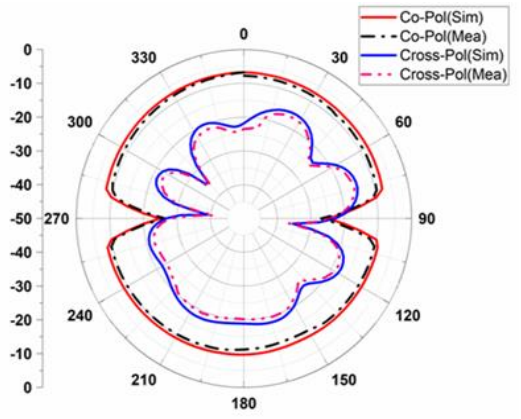

E -Plane

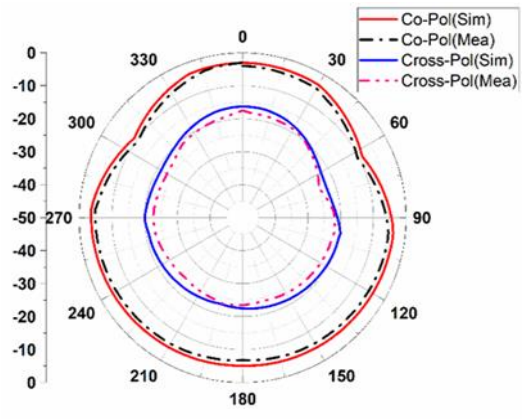

H-Plane

(a)

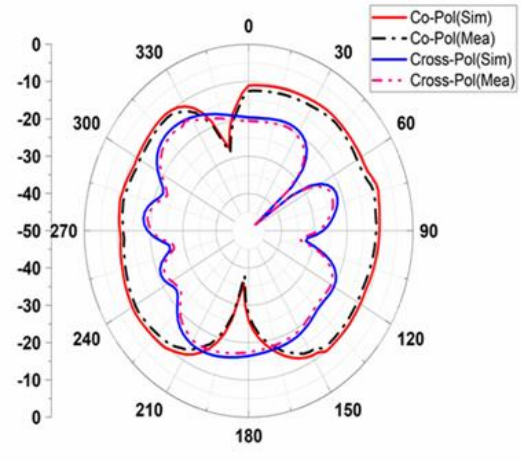

E- Plane

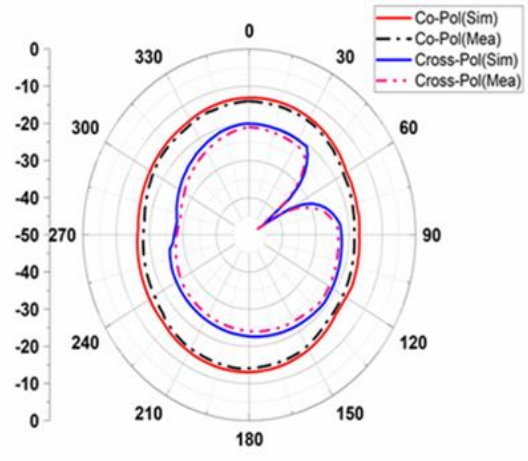

H- Plane

(b)

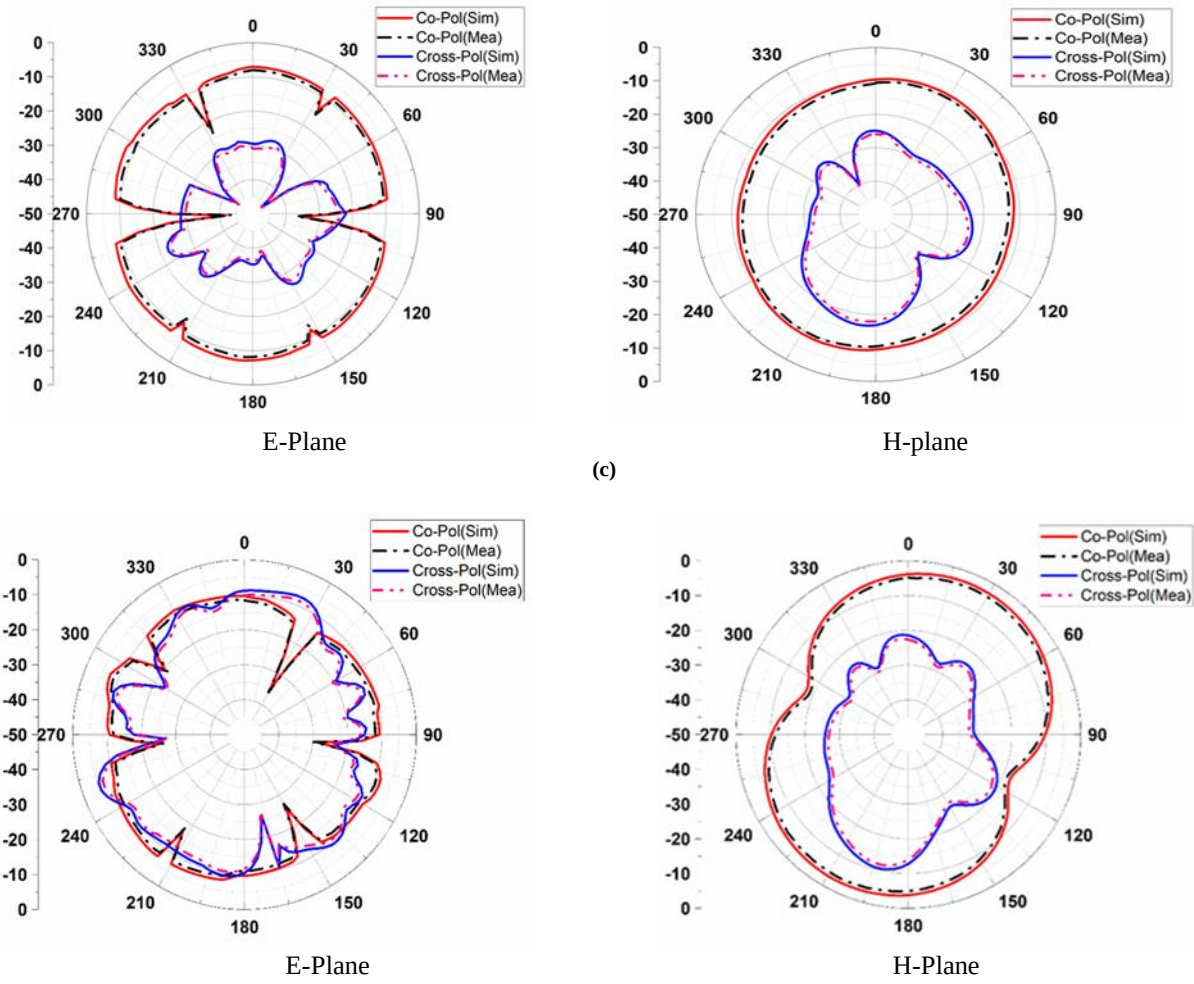

Fig. 10 The radiation characteristics at (a) 3.6GHz, (b) 5.4GHz, (c) 8.8GHz, and (d) 10.6GHz.

5.4. Quantitative Analysis of the Fabricated Antenna

Quantitative analysis of fabrication loss of quad-band MIMO antenna during the design phase, which is comprised of assessing material waste, energy consumption, yield loss, and design complexity, is discussed in this section.

Raw materials such as copper and PCB material are used in the manufacturing of the antenna but it is found that 20-25% of material is wasted in the cutting and shaping of the fabricated antenna. The fabrication process of the antenna is more complex as it consists of more resonating elements; therefore, more energy is required for testing and fabrication. Defective fabrication of the antenna due to complex design and improper impedance matching network led to yield loss, measured in percentage. Material waste, energy loss, and yield loss contribute to overall fabrication loss and more production costs.

The design complexity factor of a quad-band antenna is more than a single/two band, which leads to more manufacturing time, a larger testing period, and greater precision requirements. The impact of fabrication errors on radiation pattern or frequency response can be evaluated in terms of tolerance loss. For example, small changes in the antenna's length or placement lead to a resonant shift.

5.5. Effect of Temperature and Humidity on MIMO Antenna Performance

The design of a MIMO antenna system with low coupling is susceptible to temperature and humidity over the multi-band of the proposed antenna. The dielectric properties of materials such as substrate, foam, copper, and aluminum metal are affected by temperature variation leading to misalignment of resonant frequency and higher losses. MIMO antennas are manufactured with material that contracts and expands with temperature variation. Hence, frequency response and inter-element coupling are affected. Signal attenuation also increases with high temperatures, which impacts the quality of communication, particularly at high-frequency bands like 5G. The propagation of electromagnetic signals is also affected by temperature changes, resulting in phase shifts of signals at different frequencies.

The permittivity of dielectric material increases with a rise in humidity so that the resonant frequency of the antenna is shifted and thereby, the performance of the antenna is degraded. Higher humidity will lead to oxidation or corrosion of metallic parts such as radiating elements and feed lines. Corrosion will result in higher losses, degraded isolation, and reduced efficiency. Mutual coupling in the MIMO system is also affected by more humidity.

Temperature compensation methods are suggested to mitigate the effect of temperature variation. A temperature-compensating material with a low-temperature coefficient and electronic tuning using a varactor diode and PIN diode technique are proposed to adjust resonant frequency dynamically. MIMO antennas are protected from high humidity by using a moisture-resistant coating. Humidity-resistant substrates are used in the antenna design to ensure their dielectric properties remain stable over changing humidity conditions.

6. Statistical Significance of ECC and DG

Envelope correlation coefficient: measures the correlation between the amplitude (envelope) of signals received in a MIMO antenna system. Signals are more independent, and a lower value of ECC leads to improved diversity performance. Null hypothesis such as Pearson correlation testing is used to check whether the received signals are independent or not. Similarly, other techniques, such as P value and confidence interval, are used to measure the correlation of signals. If the value of ECC < 0.5, then antennas are not correlated, and system diversity gain is improved; otherwise, for the values of ECC greater than 0.5, system performance is degraded.

Diversity Gain: The statistical significance of diversity gain is evaluated regarding system performance metrics such as Signal-To-Noise Ratio (SNR) improvement, Bit Error Rate (BER) reduction and probability of outage obtained by multiple signal paths compared to a single antenna system. Diversity gain metrics are compared using statistical tests, such as ANOVA or t-test, to determine whether the difference between the baseline system and diversity system is statistically significant or not. Practically, simulations are often used to model different environments, such as fading and interference, and Monte Carlo simulations can estimate the probability distribution of diversity gain. Statistical significance can then be assessed through confidence intervals, variance reduction, or hypothesis testing.

High Diversity Gain and Low ECC: If the ECC between the amplitudes of the received signals at the antennas is low, then the signals are not highly correlated. Therefore, the diversity gain will be higher when the signals from different antennas are statistically independent. If the ECC is high, the signals are correlated, which limits the diversity gain. In this case, the statistical significance of diversity gain is reduced because the channels at different antennas do not offer truly independent paths for the signal.

6.1. Evaluation and Analysis of Heterogeneity Performance

The heterogeneity performance depends on the correlation among MIMO antenna elements and should be less than 0.5. Mathematically, the correlation coefficient (ρ12) is defined by Equation (5) in the form of the S specifications of the antenna. The measured ECC is < 0.0001 over the 3.1-12GHz. The calibrated and simulated ECC outcomes are compared over the 10dB bandwidth, as plotted in Figure 11(a).

$$\rho_{12} = \frac{|\, S_{11}^{*} S_{12} + S_{21}^{*} S_{22} \,|^2}{(1-(|\, S_{11} \,|^2 + |\, S_{21} \,|^2))\,(1-(|\, S_{22} \,|^2 + |\, S_{12} \,|^2))} \quad (5)$$

Mathematically, the diversity gain is defined by Equation (6) as a correlation coefficient. The diversity gain is > 9.90 dB over 3.0-12GHz. In Figure 11(b), the calibrated and simulated outcomes are compared and found to be in better agreement.

$$DG = 10*\sqrt{1 - |\, \rho_{12} \,|} \quad (6)$$

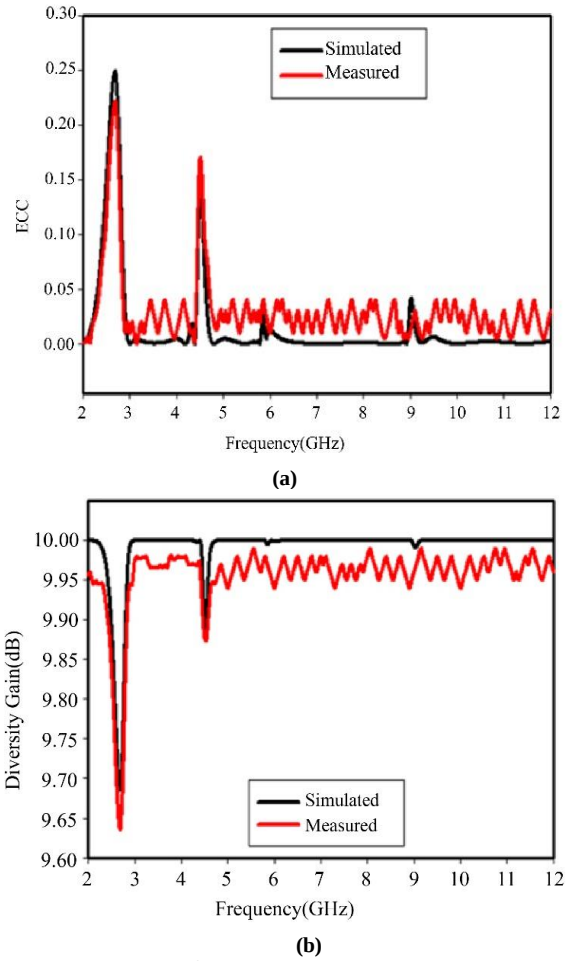

Fig. 11 Diversity performance (a) ECC, and (b) Diversity gain.

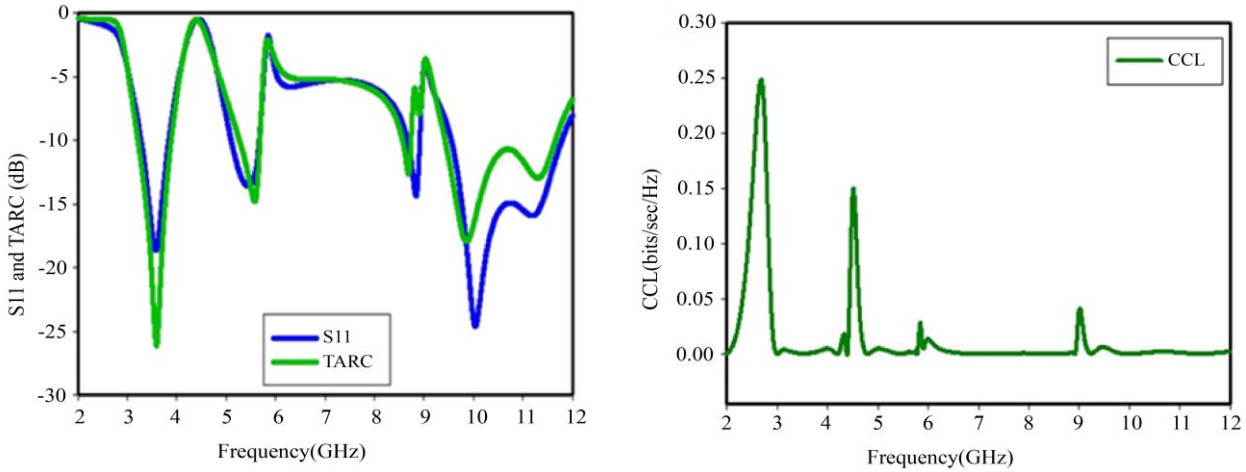

(a) **(b)**

Fig. 12 (a) TARC, and (b) CCL.

Figure 12 (a) depicts the comparison of TARC and S11. TARC < -10 dB over the quad-band of the proposed structure as given by Equation (7),

$$\Gamma_{12} = \sqrt{\frac{(S_{11} + S_{12})^2 + (S_{21} + S_{22})^2}{2}} \quad (7)$$

Γ12 represents the TARC of the antenna. The channel capacity loss must be smaller than 0.4bps/Hz. However, the CCL of the antenna is < 0.0005 bps/Hz over 3.1-12GHz, as depicted in Figure 12 (b).

6.2. Peak Gain

The peak gain changes from 1dBi to 5.83dBi over the operating spectrum 3.1-12GHz. The calibrated and actual gain are compared, and it is observed that both results are in close approximation over the working bandwidth of the antenna, as depicted in Figure 13.

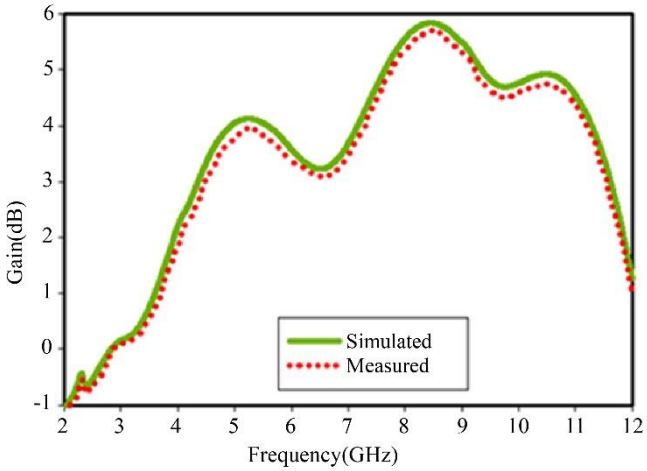

Fig. 13 Peak gain

6.3. Broadband vs Multiband of the Antenna

Broadband provides high-speed internet access with a data transmission rate of 10 Gb/sec over a wide bandwidth. Broadband connection services are of an uninterrupted type compared to previous dial-ups. Coaxial cable, fiber optics, and wireless broadband technologies are used for accessing internet services. The proposed antenna operates over multiband which covers Wi-Max, WLAN, and X band frequency range. The antenna can switch among different bands depending on the signal strength and network conditions. Better network coverage and signal strength are advantages of multiband systems. The proposed antenna is truly applicable for a multiband operation that connects to different network technologies, such as 4G and 5G. The designed antenna covers the X band (8.60-11.80GHz) with wide bandwidth; therefore, it is suitable for wireless broadband communication.

7. Analysis of Quad-Band MIMO Antenna Performance with Published Research Work

The benchmarking results of the recommended antenna are differentiated from the published literature based on multi-band, and their isolation, isolation techniques, and antenna size are tabulated in Table 3. The designed structure is compact and has a quad-band over the ultra-wideband frequency spectrum with improved isolation > 18 dB.

7.1. Practical Application of the Proposed Antenna

1. Wi-Max applications are designed in 3.2-3.8GHz frequency.
2. Massive MIMO Base Station for Wi-Max applications is designed at 3.7GHz (3.2 -3.8GHz) frequency.
3. A 5.1-5.65GHz frequency band is commonly preferred for Wi-Fi networks (IEEE 802.11ac/ax).
4. The 5G NR (New Radio) network utilizes a 5.1-5.65GHz frequency range for enhanced mobile broadband services.
5. Satellite television, radio services, and broadband services are provided over 8-12GHz frequency.
6. RADAR applications for Civilian and Military are designed in the 8-12GHz frequency range.

7. Emerging 5G networks provide high-speed wireless services over 8 -12GHz.
8. Remote sensing, such as earth observation and environmental monitoring applications, are designed over 8-12GHz frequency.

7.2. Future Work Suggestions

The proposed quad-band MIMO antenna with low coupling can find potential improvements in future research work. Firstly, we can use another decoupling technique, such as a metamaterial array, by changing the orientation of the MIMO antenna. A metamaterial-based MIMO antenna with low coupling is designed to improve the antenna's gain. K_u and K band applications can be integrated into the proposed antenna to develop Radar and Satellite communication applications. MIMO antennae are designed for ultra-wideband applications covering high-wide bandwidth over 3.1-10.6GHz. Electromagnetic interference among the different bands over ultra-wideband frequency can be minimized by designing a single/dual/triple band-notched UWB MIMO antenna with low coupling. Similarly, multiple-input-multiple-output antenna design research with enhanced isolation can be extended for millimeter wave applications at 28/38GHz.

Table 3. Comparison and analysis between a presented antenna and the literature

Ref.	10dB Bandwidth (GHz)	S21 (dB)	Isolation Techniques	Overall Size (mm^2)
[1]	3.0-3.96, 6.2-9.83, 10-16	> 16	Modified IDC	50 x 30
[2]	1.95-2.5, 3.15-3.85, 4.95-6.6	> 17	SRR	39 x 39
[4]	3.11-5.15, 4.81-7.39	> 19.5, > 21	Defected Ground Structure	35 x 30
[5]	2.04-2.51, 4.43-5.35, 6.76-8.78	> 20	Ground stub	60 x 60
[6]	2.38-2.52, 3.28-3.63, 5.05-6.77	> 18.2, >16.3, >17.1	Neutralisation line	56 x 30
[7]	2.32-2.48, 4.92-5.82	> 25.3	Meandering line resonator	60 x 60
[8]	2.38-2.52, 3.19-6.44	> 15	Orthogonal placement of Antenna	42 x 62
[10]	3.2-3.7, 5.1-5.6, 6.7-7.5	> 20	Neutralization line and slits	70 x 50
[11]	3.10-3.19, 6.11-6.43, 7.5-8.04	> 40	Dumb-bell structure	40 x 40
[12]	3.72-3.82, 4.65-4.76, 6.16-6.46	> 16	Common shared ground	32 x 32
[18]	2.37-2.64, 3.39-3.58, 4.86-6.98	> 15	Strip and open-ended slot	25 x 45
[20]	3.42-3.6, 4.7-5.1	> 28, > 44	Split EBG structure	58 x 44
[22]	2.36-2.68, 4.81-5.95	> 24, > 27	DGS and parasitic elements	50 x 30
[27]	2.4-2.52, 3.66-4, 4.62-5.52	> 30	Orientation	23.5 x 83
PO	3.25-3.85, 5.10-5.65, 8.60-8.90, 9.55-11.80	> 18	T shaped stub	44 x 20

PO = Proposed Outcome.

8. Conclusion

The paper proposed and investigated a compact MIMO antenna with poor correlation and coupling for multi-band applications. Quad-bands are achieved at 3.25-3.85GHz, 5.10-5.65GHz, 8.60-8.90GHz, and 9.55-11.80GHz over the 3.1-12GHz frequency. Improved isolation > 18dB over the 10 dB bandwidth of the antenna is obtained by loading stubs of T-shape in the ground. Moreover, correlation coefficient < 0.0001, diversity gain > 9.90dBi, the peak gain of 4.83dBi, TARC< -10dB, and CCL< 0.0005bps/Hz are achieved over the 10 dB bandwidth of the antenna.

The differentiation between calibrated and simulated outcomes shows that they correlate better over the 3.1-10.6GHz. Therefore, the miniaturized MIMO antenna is eligible for multi-band applications.

References

[1] Amit Kumar et al., "Design of Triple-Band MIMO Antenna with One Band-Notched Characteristic," *Progress in Electromagnetics Research C*, vol. 86, pp. 41-53, 2018. [CrossRef] [Google Scholar] [Publisher Link]

[2] Anitha Ramachandran et al., "A Compact Triband Quad-Element MIMO Antenna Using SRR Ring for High Isolation," *IEEE Antennas and Wireless Propagation Letters*, vol. 16, pp. 1409-1412, 2016. [CrossRef] [Google Scholar] [Publisher Link]

[3] Payam Beigi et al., "A Tiny EBG-Based Structure Multiband MIMO Antenna with High Isolation for LTE/WLAN and C/X Bands Applications," *International Journal of RF and Microwave Computer-Aided Engineering*, vol. 30, no. 3, 2020. [CrossRef] [Google Scholar] [Publisher Link]

[4] Ashim Kumar Biswas, and Ujjal Chakraborty, "Reconfigurable Wide Band Wearable Multiple Input Multiple Output Antenna with Hanging Resonator," *Microwave and Optical Technology Letters*, vol. 62, no. 3, pp. 1352-1359, 2020. [CrossRef] [Google Scholar] [Publisher Link]

[5] Ashim Kumar Biswas et al., "Compact MIMO Antenna with High Port Isolation for Triple-Band Applications Designed on a Biomass Material Manufactured with Coconut Husk," *Microwave and Optical Technology Letters*, vol. 62, no. 12, pp. 3975-3984, 2020. [CrossRef] [Google Scholar] [Publisher Link]

[6] Chengzhu Du et al., "A Compact CPW-Fed Triple-Band MIMO Antenna with Neutralization Line Decoupling for WLAN/WiMAX /5G Applications," *Progress in Electromagnetics Research M*, vol. 103, pp. 129-140, 2021. [CrossRef] [Google Scholar] [Publisher Link]

[7] Jing Ya Deng et al., "A Dual-Band MIMO Antenna Decoupled by a Meandering Line Resonator for WLAN Applications," *Microwave and Optical Technology Letters*, vol. 60, no. 3, pp. 759-765, 2018. [CrossRef] [Google Scholar] [Publisher Link]

[8] Irem Desde, Goksenin Bozdag, and Alp Kustepeli, "Multi-Band CPW fed MIMO Antenna for Bluetooth, WLAN, and WiMAX Applications," *Microwave and Optical Technology Letters*, vol. 58, no. 9, pp. 2182-2186, 2016. [CrossRef] [Google Scholar] [Publisher Link]

[9] Guo-Sheng Lin et al., "Isolation Improvement in UWB MIMO Antenna System Using Carbon Black Film," *IEEE Antennas and Wireless Propagation Letters*, vol. 16, pp. 222-225, 2016. [CrossRef] [Google Scholar] [Publisher Link]

[10] K.B.V. Babu, and B. Anuradha, "Tri-Band MIMO Antenna for WLAN, WiMAX and Defence System & Radio Astronomy Applications," *Advanced Electromagnetics*, vol. 7, no. 2, pp. 60-67, 2018. [CrossRef] [Google Scholar] [Publisher Link]

[11] Kommanaboyina Vasu Babu, and Bhuma Anuradha, "Analysis of Multi-Band Circle MIMO Antenna Design for C-Band Applications," *Progress in Electromagnetics Research C*, vol. 91, pp. 185-196, 2019. [CrossRef] [Google Scholar] [Publisher Link]

[12] R. Krishnamoorthy et al., "4 Element Compact Triple Band MIMO Antenna for Sub-6 GHz 5G Wireless Applications," *Wireless Networks*, vol. 27, pp. 3747-3759, 2021. [CrossRef] [Google Scholar] [Publisher Link]

[13] Rohit Mathur, and Santanu Dwari, "Compact CPW-Fed Ultrawideband MIMO Antenna Using Hexagonal Ring Monopole Antenna Elements," *AEU - International Journal of Electronics and Communications*, vol. 93, pp. 1-6, 2018. [CrossRef] [Google Scholar] [Publisher Link]

[14] Pasumarthi Srinivasa Rao, Jagadeesh Babu Kamili, and Avala Mallikarjuna Prasad, "Compact Multi-Band MIMO Antenna with Improved Isolation," *Progress in Electromagnetics Research M*, vol. 62, pp. 199-210, 2017. [CrossRef] [Google Scholar] [Publisher Link]

[15] Negin Pouyanfar et al., "A Compact Multi-Band MIMO Antenna with High Isolation for C and X Bands Using Defected Ground Structure," *Radioengineering*, vol. 27, no. 3, pp. 686-693, 2018. [CrossRef] [Google Scholar] [Publisher Link]

[16] Pratima Chabbilal Nirmal et al., "A Compact MIMO Antenna with Improved Isolation for 3G, 4G, Wi-Fi, Bluetooth and UWB Applications," *Progress in Electromagnetics Research C*, vol. 76, pp. 87-98, 2017. [CrossRef] [Google Scholar] [Publisher Link]

[17] Rupak Kumar Gupta, T. Shanmuganantham, and R. Kiruthika, "A Staircase Hexagonal Shaped Microstrip Patch Antenna for Multiband Applications," *International Conference on Control, Instrumentation, Communication and Computational Technologies*, Kumaracoil, India, pp. 298-303, 2016. [CrossRef] [Google Scholar] [Publisher Link]

[18] Sourav Nandi, and Akhilesh Mohan, "CRLH Unit Cell Loaded Triband Compact MIMO Antenna for WLAN/WiMAX Applications," *IEEE Antennas and Wireless Propagation Letters*, vol. 16, pp. 1816-1819, 2017. [CrossRef] [Google Scholar] [Publisher Link]

[19] Koduri Sreelakshmi, and Gottapu Sasibhushana Rao, "Reconfigurable Quad-Band Antenna for Wireless Communication," *Journal of Electrical Engineering & Technology*, vol. 15, pp. 2239-2249, 2020. [CrossRef] [Google Scholar] [Publisher Link]

[20] K. Sumathi, and M. Abirami, "Hexagonal Shaped Fractal MIMO Antenna for Multiband Wireless Applications," *Analog Integrated Circuits and Signal Processing*, vol. 104, pp. 277-287, 2020. [CrossRef] [Google Scholar] [Publisher Link]

[21] Wenjing Wu, Bo Yuan, and Aiting Wu, "A Quad-Element UWB-MIMO Antenna with Band-Notch and Reduced Mutual Coupling Based on EBG Structures," *International Journal of Antennas and Propagation*, vol. 2018, no. 1, pp. 1-10, 2018. [CrossRef] [Google Scholar] [Publisher Link]

[22] Wenying Wu et al., "A Compact Multiband MIMO Antenna for IEEE 802.11 a/b /g /n Applications," *Progress in Electromagnetics Research Letters*, vol. 84, pp. 59-65, 2019. [CrossRef] [Google Scholar] [Publisher Link]

[23] Xiaohua Tan et al., "Enhancing Isolation in Dual-Band Meander-Line Multiple Antenna by Employing Split EBG Structure," *IEEE Transactions on Antennas and Propagation*, vol. 67, no. 4, pp. 2769-2774, 2019. [CrossRef] [Google Scholar] [Publisher Link]

[24] Xiongwen Zhao, Sharjeel Riaz, and Suiyan Geng, "A Reconfigurable MIMO/UWB MIMO Antenna for Cognitive Radio Applications," *IEEE Access*, vol. 7, pp. 46739-46747, 2019. [CrossRef] [Google Scholar] [Publisher Link]

[25] Yi Zhao et al., "A Compact Dual Band-Notched MIMO Diversity Antenna for UWB Wireless Applications," *Progress in Electromagnetics Research C*, vol. 89, pp. 161-169, 2019. [CrossRef] [Google Scholar] [Publisher Link]

[26] Yue Gao et al., "Stacked Patch Antenna with Dual-Polarization and Low Mutual Coupling for Massive MIMO," *IEEE Transactions on Antennas and Propagation*, vol. 64, no. 10, pp. 4544-4549, 2016. [CrossRef] [Google Scholar] [Publisher Link]

[27] Dhanasekaran Dileepan, Somasundaram Natarajan, and Rengasamy Rajkumar, "A High Isolation Multiband MIMO Antenna without Decoupling Structure for WLAN/WiMAX /5G Applications," *Progress in Electromagnetics Research C*, vol. 112, pp. 207-219, 2021. [CrossRef] [Google Scholar] [Publisher Link]

[28] Ammar Armghan et al., "Design and Fabrication of Compact, Multiband, High Gain, High Isolation, Metamaterial-Based MIMO Antennas for Wireless Communication Systems," *Micromachines*, vol. 14, no. 2, pp. 1-20, 2023. [CrossRef] [Google Scholar] [Publisher Link]

[29] Daud Khan, Ashfaq Ahmad, and Dong-You Choi, "Dual-Band 5G MIMO Antenna with Enhanced Coupling Reduction Using Metamaterials," *Scientific Reports*, vol. 14, no. 1, pp. 1-16, 2024. [CrossRef] [Google Scholar] [Publisher Link]